

To the editor:

The JAK-STAT signaling pathway is differentially activated in *CALR*-positive compared with *JAK2V617F*-positive ET patients

Philadelphia chromosome–negative myeloproliferative neoplasms (MPNs), including polycythemia vera, essential thrombocythemia (ET), and primary myelofibrosis, are clonal hematopoietic stem cell disorders frequently associated with a somatic *JAK2V617F* mutation.¹ The gain-of-function *JAK2V617F* mutation is associated with ligand-independent activation of cytokine signaling pathways. Tyrosine phosphorylation and activation of signal transducer and activator of transcription 5 (STAT5) and STAT3 appear to play a central role in MPN pathogenesis.²

Two independent studies reported recurrent mutations of the *CALR* gene in the majority of *JAK2* wild-type ET and primary myelofibrosis patients.^{3,4} *JAK2* and *CALR* mutations are often mutually exclusive, suggesting that the latter may also activate cytokine signaling. Indeed, expression of mutant *CALR* in Ba/F3 cells was reported to result in cytokine-independent proliferation with increased phospho-STAT5 expression and sensitivity to *JAK2* inhibition.⁴ However, these data contrast with the observation that MARIMO cells, derived from an ET patient harboring an endogenous *CALR* mutation, contain very low levels of tyrosine-phosphorylated and unphosphorylated *JAK2* and STAT5, and are insensitive to *JAK2* inhibition.⁵

Rampal et al subsequently reported in this journal that a gene expression signature of *JAK2* activation is shared by peripheral blood granulocytes from *JAK2*-mutant and *CALR*-mutant MPN patients.⁶ Microarray gene expression data for 93 MPN patients and 11 age-matched controls were described, providing a valuable resource for the MPN field.⁶ Gene set enrichment analysis (GSEA) was used to propose that similar JAK-STAT transcriptional profiles were induced in *JAK2*-mutant and *CALR*-mutant patients.⁶

GSEA is a widely used tool for analyzing microarray data. However, one drawback is that it relies on predefined gene sets often produced from published information or collected from other databases.⁷ The availability of biologically relevant data sets for GSEA is therefore a limitation to an otherwise powerful analytical tool. Rampal et al used RNA interference–mediated knockdown of *JAK2* in the *JAK2V617F* short hairpin RNA knockdown signature, which was enriched to a similar extent in *JAK2*-mutant and *CALR*-mutant patients.⁶ Their conclusion that both groups of patients also shared a STAT signature was based on the use of a previously published data set of genes differentially expressed between in vitro–differentiated wild-type mouse embryonic stem cells and embryonic stem cells overexpressing STAT5A protein.⁸ Constitutively active STAT5A in this system is expressed from day 0 and therefore many of the expression differences identified by microarray analysis of day 5 cells may be due to indirect effects.⁸

Recently, we have identified direct STAT targets that are activated in primary in vitro–cultured human megakaryocytes by performing genome-wide chromatin immunoprecipitation sequencing (ChIP-seq) analysis for phosphorylated STAT3 and STAT5 following thrombopoietin (TPO) stimulation (Figure 1A-B; unpublished data). This created an opportunity to use these gene sets, derived from a cell type central to MPN pathogenesis, to reevaluate the gene expression data presented by Rampal and colleagues (Figure 1C-D).

Using GSEA, we see markedly different STAT activation signatures between *JAK2*-mutant and *CALR*-mutant ET patients (Figure 1D). Overlapping subsets of direct STAT1 and STAT3 targets were induced in *JAK2*-, but not in *CALR*-mutant, patients when compared

with normal controls. Gene ontology analysis of induced genes revealed contrasting biological processes, with the JAK-STAT cascade enriched in *JAK2*-mutant patients, whereas response to unfolded protein genes was enriched in *CALR*-mutant patients. To corroborate that genes enriched in *JAK2*-mutant patients, when compared with *CALR*, are JAK-activated STAT targets, we performed gene ontology analysis on the leading-edge genes shared between the 2 megakaryocyte phospho-STAT datasets used in GSEA, which identified JAK-STAT signaling as the top enriched pathway and included several paradigmatic JAK-STAT targets.

GSEA is critically dependent on the availability of biologically relevant gene sets. Our results demonstrate that direct STAT3 and STAT5 target genes, identified by ChIP-seq studies of a cell type central to ET pathogenesis (megakaryocytes), are upregulated in cells from *JAK2*- but not *CALR*-mutant ET patients. Therefore, although we concur with Rampal and colleagues that a *JAK2* activation signal may be present in *CALR*-mutant ET granulocytes, our results indicate that downstream signaling mechanisms other than STAT3 and STAT5 are likely involved in the pathogenesis of *CALR*-mutant MPNs. Comparative analysis of normal and ET-derived primary megakaryocytes will likely be required to fully resolve potential differences in pathologic signaling between *JAK2*- and *CALR*-mutant MPNs.

Winnie W. Y. Lau

Cambridge Institute for Medical Research and
Wellcome Trust/Medical Research Council,
Stem Cell Institute and Department of Haematology,
University of Cambridge,
Cambridge, United Kingdom

Rebecca Hannah

Cambridge Institute for Medical Research and
Wellcome Trust/Medical Research Council,
Stem Cell Institute and Department of Haematology,
University of Cambridge,
Cambridge United Kingdom

Anthony R. Green

Cambridge Institute for Medical Research and
Wellcome Trust/Medical Research Council,
Stem Cell Institute and Department of Haematology,
University of Cambridge,
Cambridge, United Kingdom
Department of Haematology,
Addenbrooke's Hospital,
Cambridge, United Kingdom

Bertie Göttgens

Cambridge Institute for Medical Research and
Wellcome Trust/Medical Research Council,
Stem Cell Institute and Department of Haematology,
University of Cambridge,
Cambridge, United Kingdom

Acknowledgments: Samples were provided by the Cambridge Blood and Stem Cell Biobank, which is supported by the Cambridge National Institute for Health Research Biomedical Research Centre and the Cambridge Experimental Cancer Medicine Centre. Approval was obtained from Cambridge University Hospitals NHS Foundation Trust for these studies. Informed consent was provided according to the Declaration of Helsinki. Work in A.R.G.'s and B.G.'s laboratories is supported by the Biotechnology and Biological Sciences Research Council, the Medical Research Council, Leukemia and Lymphoma Research, Cancer Research UK, the Leukemia and Lymphoma Society of America, the Cambridge National Institute for Health Research Biomedical Research Centre,

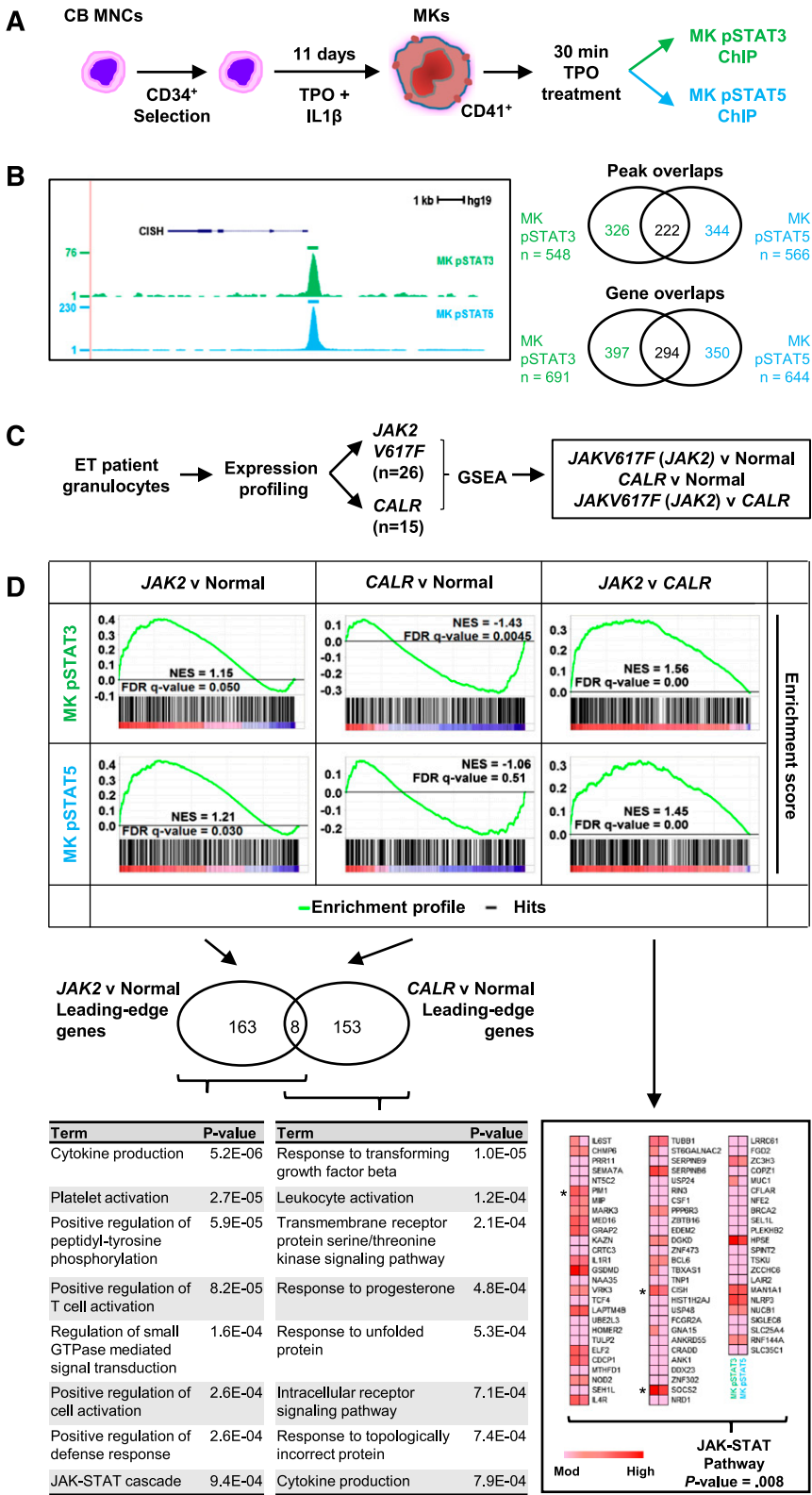


Figure 1. Megakaryocytic STAT targets are enriched in granulocytes from ET *JAK2*-mutant patients but not ET *CALR*-mutant patients. (A) Schematic of megakaryocyte (MK) cells derived from cord blood (CB) mononuclear cells (MNCs). After an 11-day culture in stem cell growth media (SCGM, Cell Genix) supplemented with 100 ng/mL TPO (Cell Genix) and 10 ng/mL interleukin-1β (IL-1β, Miltenyi), mature MK cells were treated with 50 ng/mL TPO for 30 minutes and used for ChIP with pSTAT3 and pSTAT5 antibodies (Cell Signaling Technologies). (B) Example of a density plot transformed from raw ChIP-seq data reads, displayed in the UCSC Genome Browser. *CISH* gene structure is shown above the tracks. Venn diagrams depict peak and gene overlaps from ChIP-seq data. Genomic coordinates of STAT-bound peaks were converted to gene lists using UCSC as the gene source. (For a complete list of STAT-bound peaks and genes, see supplementary Tables 1 and 2). (C) ET patient granulocytes were genotyped and expression-profiled by Rampal et al⁶; samples that were independently positive for *JAK2V617F* and *CALR* were processed in GSEA⁷ with pSTAT3 and pSTAT5 ChIP-Seq data sets from TPO-treated MK cells. (D) GSEA results showing activated STAT signatures enriched in ET patients with *JAK2V617F (JAK2)* mutation relative to both normal and ET patients positive for *CALR* mutation (*CALR*). All 3 GSEA comparisons (*JAK2* vs normal, *CALR* vs normal and *JAK2* vs *CALR*) were evaluated with leading-edge analysis (see supplementary Table 3) to determine which genes contributed to the normalized enrichment score (NES).⁷ Leading-edge genes are core-enriched genes that are ordered in a ranked gene list (as depicted as black and white bars below a GSEA profile) and appear at, or before, an automatically generated enrichment score threshold.⁷ Gene ontology analysis was performed for leading-edge genes using Enrich⁹ and the Functional Annotation tool of the Database for Annotation, Visualization and Integrated Discovery¹⁰, version 6.7 (david.abcc.ncicrf.gov). Nonredundant gene ontology biological process terms with *P* values < .001 are shown below a Venn diagram of leading-edge genes enriched in *JAK2*-mutant patients compared with controls, and *CALR*-mutant patients compared with controls (for full gene ontology biological process table of terms, see supplementary Tables 4-6). For GSEA comparing *JAK2* against *CALR* patients, the 76 leading-edge genes shared by both pSTAT ChIP-seq datasets in MK cells are also shown as a heat map indicating relative expression. Gene expression is denoted pink to red, indicating moderate (mod) to high expression. Gene ontology analysis of these 76 shared leading-edge genes was performed and the main Kyoto Encyclopedia of Genes and Genomes pathway is depicted. *Key canonical JAK-STAT target genes. All *P* values shown were evaluated by the modified Fisher's exact test. FDR, false discovery rate; GTPase, guanosine triphosphatase. All supplementary tables are freely available at http://hsc1.cimr.cam.ac.uk/genomic_supplementary.html.

and the Kay Kendall Leukaemia Fund (A.R.G.). Infrastructure funding was provided by the Wellcome Trust-Medical Research Council Cambridge Stem Cell Institute.

Contribution: W.W.Y.L. performed experiments, produced the figure and wrote the manuscript. W.W.Y.L. and R.H. performed data analysis. W.W.Y.L., B.G., and A.R.G. interpreted the data. B.G. and A.R.G. edited the manuscript. All authors read and approved the paper.

Conflict-of-interest disclosure: The authors declare no competing financial interests.

Correspondence: B. Göttgens, Cambridge Institute for Medical Research, Hills Road, Cambridge, CB2 0XY, UK; e-mail: bg200@cam.ac.uk; and A. R. Green, Cambridge Institute for Medical Research, Hills Road, Cambridge, CB2 0XY, UK; e-mail: arg1000@cam.ac.uk.

References

- Pasquier F, Cabagnols X, Secardin L, Plo I, Vainchenker W. Myeloproliferative neoplasms: JAK2 signaling pathway as a central target for therapy. *Clin Lymphoma Myeloma Leuk*. 2014;14(suppl):S23-S35.
- Chen E, Staudt LM, Green AR. Janus kinase deregulation in leukemia and lymphoma. *Immunity*. 2012;36(4):529-541.
- Klampfl T, Gisslinger H, Harutyunyan AS, et al. Somatic mutations of calreticulin in myeloproliferative neoplasms. *N Engl J Med*. 2013;369(25):2379-2390.
- Nangalia J, Massie CE, Baxter EJ, et al. Somatic CALR mutations in myeloproliferative neoplasms with nonmutated JAK2. *N Engl J Med*. 2013;369(25):2391-2405.
- Kollmann K, Nangalia J, Warsch W, et al. MARIMO cells harbor a CALR mutation but are not dependent on JAK2/STAT5 signaling [letter]. *Leukemia*. 2015;29(2):494-497.
- Rampal R, Al-Shahrour F, Abdel-Wahab O, et al. Integrated genomic analysis illustrates the central role of JAK-STAT pathway activation in myeloproliferative neoplasm pathogenesis. *Blood*. 2014;123(22):e123-e133.
- Subramanian A, Tamayo P, Mootha VK, et al. Gene set enrichment analysis: a knowledge-based approach for interpreting genome-wide expression profiles. *Proc Natl Acad Sci USA*. 2005;102(43):15545-15550.
- Schuringa JJ, Wu K, Morrone G, Moore MA. Enforced activation of STAT5A facilitates the generation of embryonic stem-derived hematopoietic stem cells that contribute to hematopoiesis in vivo. *Stem Cells*. 2004;22(7):1191-1204.
- Chen EY, Tan CM, Kou Y, et al. Enrichr: interactive and collaborative HTML5 gene list enrichment analysis tool. *BMC Bioinformatics*. 2013;14(128):128.
- Huang W, Sherman BT, Lempicki RA. Systematic and integrative analysis of large gene lists using DAVID bioinformatics resources. *Nat Protoc*. 2009;4(1):44-57.

© 2015 by The American Society of Hematology

To the editor:

An analysis of the thromboembolic outcomes of 2472 splenectomized individuals

The diseases associated with the reason for splenectomy play an important role in the rate of infections in splenectomized patients.¹ Our hypothesis was that the same reasoning would apply to the rates of venous thromboembolism (VTE) after splenectomy and that these findings could inform future preventive care.

All patients undergoing a splenectomy in Victoria, Australia, were identified by using linked hospital discharge data with International Classification of Diseases, 10th Revision, Australian Modification (ICD-10-AM) diagnostic codes.² The sampling frame included patients between July 1, 1998, and December 31, 2006, who were ≥15 years of age. This sampling frame was selected to ensure adequate numbers of patients in each of the splenectomy indication groups for statistical power. Splenectomy indications were divided into 6 mutually exclusive groups, and patients who had multiple indications were ordered hierarchically: (1) trauma, (2) therapeutic malignant (planned; malignant disease such as lymphoma or leukemia), (3) therapeutic hematologic (planned; hematologic disease such as idiopathic thrombocytopenic purpura [ITP] or hemolytic

anemia), (4) therapeutic other (local infections or congenital abnormalities of the spleen), (5) iatrogenic malignant (unplanned; unintended accompaniment to surgery for malignant disease), and (6) iatrogenic nonmalignant (unplanned; unintended consequence of surgery for nonmalignant disease).

VTE was divided by using ICD-10-AM codes into lower-extremity acute deep vein thrombosis (DVT), pulmonary embolism (PE), and portal vein thrombosis (PVT). This classification was based on studies using similar coding methodologies.³ The groups were not mutually exclusive. Patients who had VTE that occurred in the first 30 days after splenectomy were excluded to avoid inclusion of complications potentially resulting from the primary surgery or related admission. Incidence rates of first VTE were calculated for sex, age group, and indication for splenectomy. Multivariate Cox proportional hazards regression models were fitted to compute hazard ratios adjusted for age, sex, and indication for splenectomy. Hazards proportionality was assessed by using analysis of scaled Schoenfeld residuals. All reported *P* values were two-tailed and, for each analysis, *P* < .05 was considered significant. We used Stata, version 131.0 (STATA,

Table 1. Adjusted rates of first VTE in splenectomized patients

	No. of patients	Events		Incidence rates per 100 person-years		Unadjusted (univariable)			Adjusted (multivariable)		
		No.	%	Value	95% CI	HR	95% CI	<i>P</i>	HR	95% CI	<i>P</i>
Sex											
Male	1325	68	5.1	1.17	0.92 to 1.48	1			1		
Female	1147	74	6.5	1.45	1.15 to 1.82	1.25	0.90 to 1.74	.179	1.17	0.84 to 1.63	.366
Age group (y)											
<50	947	27	2.9	0.62	0.42 to 0.90	1			1		
50+	1525	115	7.5	1.75	1.46 to 2.11	2.75	1.81 to 4.18	<.001	2.57	1.62 to 4.09	<.001
Splenectomy indication											
Therapeutic malignancy	269	21	7.8	1.74	1.14 to 2.67	2.23	1.23 to 4.06	.008	1.32	0.70 to 2.49	.395
Therapeutic hematologic	583	36	6.2	1.33	0.96 to 1.85	1.75	1.03 to 2.98	.038	1.28	0.74 to 2.22	.372
Therapeutic other	138	8	5.8	1.35	0.67 to 2.70	1.68	0.75 to 3.76	.211	1.38	0.61 to 3.12	.438
Iatrogenic noncancer	350	16	4.6	1.01	0.62 to 1.64	1.30	0.68 to 2.47	.426	0.80	0.41 to 1.57	.514
Iatrogenic cancer	497	39	7.9	1.89	1.38 to 2.58	2.32	1.38 to 3.91	.002	1.30	0.73 to 2.30	.371
Trauma	635	22	3.5	0.79	0.52 to 1.20	1			1		

HR, hazard ratio.